Exciton Formation and Annihilation during 1D Impact Excitation of Carbon Nanotubes

L. Marty,[1] E. Adam,[2] L. Albert,[3] R. Doyon,[3] D. Ménard,[2] and R. Martel[1,*]

[1]*Département de Chimie et Regroupement Québécois sur les Matériaux de Pointe—RQMP, Université de Montréal, Montréal QC H3T1J4, Canada*

[2]*Département de Génie Physique et Regroupement Québécois sur les Matériaux de Pointe—RQMP, Ecole Polytechnique de Montréal, Montréal QC H3T1J4, Canada*

[3]*Département de Physique, Université de Montréal, Montréal QC H3T1J4, Canada*

(Received 22 November 2005; published 4 April 2006)

Near-infrared electroluminescence was recorded from unipolar single-wall carbon nanotube field-effect transistors at high drain-source voltages. High resolution spectra reveal resonant light emission originating from the radiative relaxation of excitons rather than heat dissipation. The electroluminescence is induced by only one carrier type and ascribed to 1D impact excitation. An emission quenching is also observed at high field and attributed to an exciton-exciton annihilation process and free carrier generation. The excitons' binding energy in the order of 270 meV for 1.4 nm SWNTs is inferred from the spectral features.

DOI: 10.1103/PhysRevLett.96.136803 PACS numbers: 73.63.Fg, 78.60.Fi, 78.67.Ch, 79.20.Kz

Theory predicted first that single-wall carbon nanotubes (SWNTs) should exhibit strong electron-hole pair interactions [1–3]. This was verified using the application of selection rules to photoluminescence (PL) excitation [4,5]. The accumulated evidence of excitonic effects in SWNTs is now plentiful and it is fair to expect that excitonic transitions will dominate the optical properties of SWNTs. This should also be true for SWNT devices, but the recent experiments on SWNT photoconductivity [6,7] and electroluminescence [8–10] show mainly electro-optical responses that are similarly observed in other semiconductor devices, where excitons play no major role. High resolution data of emission and photoconductivity are required in order to gain insights into the excitonic effects and dynamics in nanotube devices.

In this Letter, we present well-resolved spectra of electroluminescence (EL) induced by high energy scattering in unipolar single-wall carbon nanotube field-effect transistors (CNFETs). We first show that the CNFETs emit light in the near-infrared (near-IR) at large drain-source voltage (V_d) and prove that impact excitation is an important mechanism for exciton creation in CNFETs. We then explore the various EL regimes at high electric field up to the device breakdown. Based on the emission spectra, we discuss on the interplay between the exciton formation, the exciton-exciton annihilation leading to EL quenching and the generation of free carriers.

The SWNTs were synthesized by laser ablation (Rice University) giving nanotube diameters of 1.4 ± 0.1 nm. CNFETs were prepared using SWNTs dispersed in 1,2-dichloroethane and spin coated on a *p*-doped oxidized silicon wafer (150 nm SiO_2). Source-drain cobalt electrodes were patterned on top of the SWNTs using optical lithography to design electrode spacings in the 500–1500 nm range [11]. The contacts were improved by H_2SO_4 treatment followed with a 400 °C anneal in argon. The CNFETs obtained by our process exhibit unipolar *p*-type behavior in air and operate with the substrate as a back gate. The devices used have rather high contact resistances, in the MΩ range, and a current modulation of a few decades, which is typical of CNFET made of small bundles of SWNTs.

The CNFETs' light emission was detected with the infrared spectrometer of Montreal (SIMON), a near-IR camera equipped with a 1024×1024 HgCdTe detector (Rockwell-Hawaii-1) and designed to fit on the Mont-Mégantic astronomical telescope (Québec, Canada) [12]. For this study, SIMON was adapted on a custom made probe station. The CNFETs are located on its focal plane and operate in air at room temperature (details in Ref. [13]). This camera has several exchangeable filters and prisms for both imaging and spectroscopic modes. In the imaging mode, two bandpass filters were used to limit the detection within the 0.70–0.84 eV (*H* filter) and 0.54–0.62 eV (*K* filter) ranges. The spectroscopic mode was set with the large bandpass Amici filter (0.52–1.55 eV, i.e., the full range of the camera) and the Amici prism to diffract the incident light over 120 pixels on the detector plane. The whole optical setup, including the filters and prisms, was kept at liquid nitrogen temperature. No warm lenses were added to the light path in order to minimize the thermal noise. As a result, the spatial resolution in the imaging mode was only 30 μm per pixel.

Typical CNFET emission image and spectrum are shown in Fig. 1. The image in the inset was acquired at $V_d = 14$ V using the *K* filter. In this detection range, the cobalt pads appear darker because of a weaker near-IR emission background compared to the SiO_2 surface, and the bright spot at the center of the image corresponds to the emission from the CNFET. A typical spectrum of a CNFET emission (Fig. 1) exhibits a sharp resonance emission peak (here centered at 0.69 eV) dominating the whole spectrum. Note

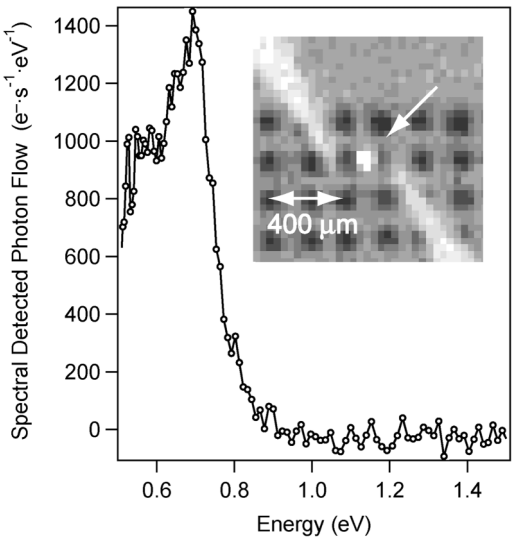

FIG. 1. Spectrum of the emitted light at $V_d = 8$ V (constant voltage mode) and $V_g = -20$ V. The integration time is 120 s. Inset: image of the emission with the K filter (2.6 s exposure) taken at constant voltages ($V_d = 14$ V, $V_g = -15$ V). The voltage probes appear as white needles and the SWNT emission as a bright spot (see arrow).

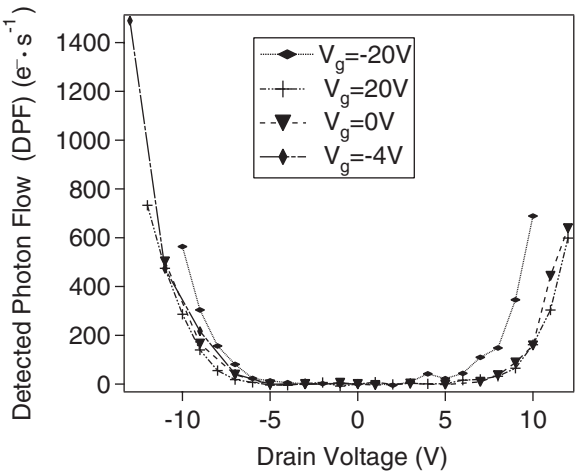

FIG. 2. Detected Photon Flow with the H filter as a function of the drain voltage for different gate voltages.

that the light spectral signal is given in units of electrons-s^{-1}-eV^{-1} collected on the detector rather than in photons-s^{-1}-eV^{-1}. The estimated collection efficiency of SIMON is $(2.6 \pm 1.1) \times 10^{-4}$ electron detected per photon [13,14]. Spectra taken at high V_d from a dozen unipolar CNFETs reveal similar emission peak profiles in the 0.5–0.8 eV energy range. Electroluminescence is observed for all devices showing conductance modulation by the gate field, but its intensity is device dependent.

Previous work already reported on optical emission from multiwall nanotube bundles stressed at high V_d [15]. The highest energy part of the spectrum was recorded and assigned to conventional blackbody radiation coming from Joule heating. The resonance in Fig. 1 at 0.69 eV cannot be assigned to local heating because the blackbody spectrum for such a peak would correspond to a local temperature of about 1700 K. SWNTs readily burn in air at such temperature.

Overall, the peak position is the same compared to the PL results from SWNT samples of similar diameter distribution [16,17] and the spectra are similar in shape and position to those obtained from ambipolar CNFETs [9]. Thus, the main emission originates from the same excited state.

The emission intensity, recorded with the H filter, is plotted for different drain-source and gate voltages (Fig. 2). The EL is systematically observed above a threshold voltage, $V_d > V_{\text{th}}$. The gate voltage (V_g) has no clear influence on the light intensity normalized by the current (not shown). This is in contrast to previous EL studies on ambipolar CNFETs [8]. The characteristics for each V_g exhibit similar voltage thresholds for light emission. Above V_{th}, the relevant parameter is V_d. For instance, the curve at $V_g = -20$ V shows the emission when only holes can physically access the nanotubes. Thus, we conclude that the mechanism for light emission above V_{th} involves mainly the excitation from a single carrier type. These conditions are different from the optimum emission conditions of ambipolar CNFETs, for which electrons and holes are injected at an equal rate from both ends of the nanotubes at $V_d = 2V_g$ [8,9].

These results support a mechanism of impact excitation, where inelastic scattering of conduction carriers effectively create free or localized excitons in the SWNT. That is, the carrier excess energy at high V_d is transferred by collisions to the valence electrons, which create excitons in the SWNT [Fig. 3(a)]. Such an excitation scheme is known in conventional semiconductors to generate exciton-mediated EL [18,19] and free carrier recombination [20,21]. In CNFETs, we detect EL without the exponential increase of the drain current usually associated with free carrier generation. Thus, CNFET emission is explained by

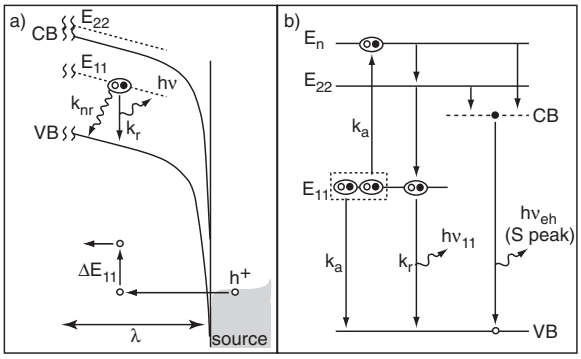

FIG. 3. (a) Model of impact excitation in CNFETs. The band structure is shown for $V_d > 0$ and $V_g < 0$. The plain arrows represent impact excitation on the first excitonic band (dotted level) (b) Model illustrating the radiative channels and exciton-exciton annihilation.

exciton formation rather than band to band ionization of free carriers.

To ensure the stability of the excitons, the thermal energy (k_BT) should be small compared to the exciton binding energy, i.e., the energy between the excitonic level ($E_{1,1}$) and the conduction band (CB) edge. In conventional semiconductors, this condition is only achieved at low temperature; the radiative regime associated with impact excitation is consequently unobservable at room temperature. In comparison, the excitonic effects are much stronger in SWNTs [1–5]: the minimum energy required to create an exciton corresponds to the energy of the transition to the first exciton state which is expected to be significantly smaller than the free electron bandgap [2]. The proposed mechanism requires that the emission spots should be located at sites where the kinetic energy distribution of free carriers is at the maximum, which is mainly determined by the accelerating field defined by the voltage drop. In our CNFETs, this is most likely located in the vicinity of the contacts, i.e., close to the metal-SWNT Schottky contact within the mean free path λ [11]. The emission sites can also correspond to strong collision sites at structural defects, bent regions, or impurities [10].

The evolution of the spectrum for another representative CNFET as a function of V_d is presented in Fig. 4. The spectra are normalized by the mean current so that the plotted signal does not depend on the number of injected carriers. As the voltage is increased above V_{th} and for a constant gate voltage, we observe 3 successive emission regimes as labeled in Fig. 4(b). *Regime 1*: the optical signal

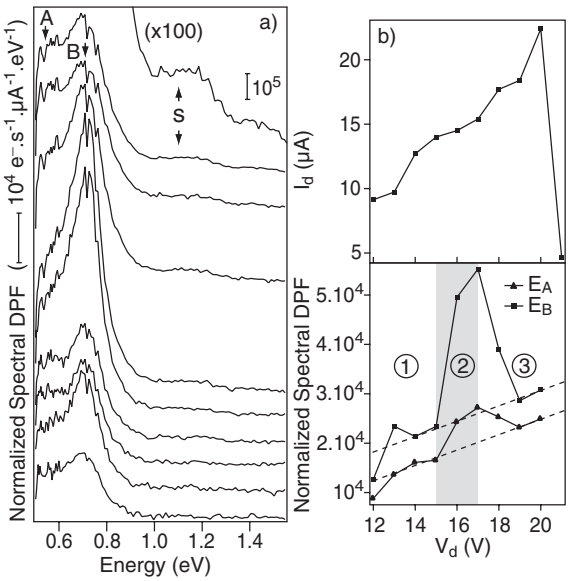

FIG. 4. (a) Evolution of the emission spectrum with the drain-source voltage ($V_d = 12$ V to 21 V from bottom to top and $V_g = -10$ V). The spectra have been normalized by the average current and vertically translated for clarity. (b) Top: Average current during each spectrum acquisition. Bottom: Light intensity extracted from the spectra at two different energies [*A* and *B* are shown in (a)].

increases with V_d and the main peak becomes gradually more pronounced [Fig. 4(a)]. *Regime 2*: at $V_d = 15$ V, a sharp increase of the emission is observed. *Regime 3*: the emission is quenched above $V_d = 17$ V, until the definitive breakdown of the device occurs at $V_d = 21$ V. These 3 regimes are better seen on Fig. 4(b) (lower panel) by plotting the normalized signal (i.e., the spectral density of photon flow) as a function of V_d for two different energy points of the spectrum, labeled *A* and *B* (see arrows). These points, $E_A = 0.55$ eV and $E_B = 0.71$ eV, correspond to the shoulder in the lowest part of the spectrum and to the resonance peak maximum, respectively. The *A* region is taken below the exciton peak and is then associated with the blackbody emission tail of the device. Although we cannot exclude possible emission contributions from strongly localized exciton states at defect sites, the intensity in *A* increases with V_d, which is a signature of local heating. The intensity of the peak at E_B dominates the total emission and follows the same background, as in *A*, due to the blackbody tail of the heat spectrum. Without this contribution, the EL in *B* appears constant in the 1st regime, i.e., simply proportional to the current. This agrees with a constant number of excitons generated per injected electron by impact excitation. The current calibration of the photon collection efficiency of our experimental setup with the observed photon count indicates that the EL efficiency corresponds to $\sim 10^{-5}$ emitted photons per injected electron. Considering that the branching ratio between radiative and nonradiative processes [See Fig. 3(a)] is about 10^{-4} in SWNTs [22,23], it is reasonable to conclude that the cross section for inelastic scattering is very high (i.e., close to 0.1).

For V_d between 15–17 V [regime 2 on Fig. 4(b)], the light intensity at E_B suddenly increases, which is not related to an increase of the current as the plotted signal is normalized by the mean value of I_d. Thus, the rate of emission at the steady state increases further to reach a maximum value that is about twice as high as before. This unexpected change fits well with a simple kinetic model where the rate of exciton formation by impact suddenly exceeds the rate of exciton relaxation (i.e., the rate of the nonradiative channels, k_{nr}) [24]. The saturation of the nonradiative channels permits a sharp increase of the exciton concentration. The presence of a threshold for multiple inelastic scattering could also contribute to the sharp increase of the exciton formation rate.

Above $V_d = 17$ V [i.e., regime 3 in Fig. 4(b)], the normalized light intensity at E_B decreases while I_d is still increasing. This quenching of EL has been observed in several CNFETs just prior to the breakdown. At this point, the concentration of excitons is the highest and a new competing nonradiative channel opens up and contributes to the annihilation of the excitons. Similar quenching of EL at high field has previously been observed in AlGaAs/GaAs quantum wells at 1.4 K and ascribed to the ionization of excitons by hot carriers [19]. However, there are good reasons to support an alternative model of

CNFET EL quenching based on exciton-exciton (ex-ex) annihilation, as presented in Fig. 3(b). This model was recently proposed by Ma and coworkers to explain PL results at high laser fluence [24]. First, excitons in SWNTs are significantly stronger than for conventional semiconductors and, as a result, their binding energy is higher. Second, fast exciton relaxation in SWNTs was recently identified during high laser fluence PL experiments [25]. Last, our estimate of the exciton concentration is high and several excitons coexist in the SWNT (the scattering cross section implies that at least 10 excitons per ps are formed by impact excitation). In fact, the ex-ex annihilation process was recently proven to dominate at high laser fluence, i.e., when the exciton concentration is high [24,26]. Regime 3 is close to the device breakdown, which occurs at $V_d = 21$ V. Thus, the underlying mechanism of ex-ex annihilation is likely to be involved during the electrical breakdown of CNFETs.

Finally, the satellite peak S identified by the arrow in Fig. 4 appears progressively during the 3rd regime. This peak is wide (FWHM = 0.24 eV), centered at 1.1 eV, redshifted by 0.1 eV relative to the $E_{2,2}$ transition expected for these SWNTs [17]. Thus, this cannot be assigned to the $E_{2,2}$ exciton state. In fact, EL from the $E_{2,2}$ state is unlikely because the lifetime is too short (i.e., tens of fs) [27] and fluorescence from this state has never been observed before. It is important to note, however, that the peak S appears during the EL quenching regime, ascribed to the ex-ex annihilation process. Emission occurring from the recombination of free electrons and holes resulting from the ex-ex annihilation has already been measured in SWNTs [26]. The process leading to this emission is illustrated in Fig. 3(b). It is therefore reasonable to conclude that this S peak is an emission feature from the recombination of free carriers. Considering the identification made of the peaks B and S in Fig. 4(a), we can use the spectrum to estimate the exciton binding energy. This value is the difference between the CB edge and the $E_{1,1}$ emission peak. The free carriers generated by the ex-ex annihilation are formed with a large excess kinetic energy due to the transition energy involving the higher E_n state. Thus, the maximum of the S peak is not the minimum of the CB. An estimate of the band edge can however be made by taking the minimum value of this peak (i.e., 0.96 eV) and compare it with the center of the excitonic $E_{1,1}$ peak. This difference is the binding energy of the exciton. A value of $\sim$270 meV is extracted, which is in good agreement with the excitonic binding energy previously measured [28]. Last, we observe a weak peak centered at $\sim$1.4 eV [see Fig. 4(a)], the origin of which is yet unclear. We speculate this is the $E_{2,2}$ free carrier recombination.

In conclusion, we have presented a complete electroluminescence study of unipolar CNFETs in the infrared region. The well-resolved spectra of EL exhibit emission peaks related to excitons and free carrier recombination. We have identified a regime of EL quenching ascribed to ex-ex annihilation, which is the main channel for the generation of the free carriers.

The authors thank S. Auvray, C. Aguirre, M. Paillet, and C. Silva for valuable discussions and Philippe Vallée (L. A. E.) for technical assistance. This project is supported by the Canada Research Chair Program (CRC), NSERC, and FQRNT (Québec).

Note added.—Just prior to the submission of this Letter, we became aware of a new paper with similar results published in Ref. [29].

*Electronic address: r.martel@umontreal.ca

[1] T. Ando, J. Phys. Soc. Jpn. **66**, 1066 (1997).
[2] C. D. Sparatu, S. Ismail-Beigi, L. X. Benedict, and S. G. Louie, Phys. Rev. Lett. **92**, 077402 (2004).
[3] V. Perebeinos, J. Tersoff, and Ph. Avouris, Phys. Rev. Lett. **92**, 257402 (2004).
[4] F. Wang, G. Dukovic, L. E. Brus, and T. F. Heinz, Science **308**, 838 (2005).
[5] S. Reich *et al.*, Phys. Rev. B **71**, 033402 (2005).
[6] M. Freitag *et al.*, Nano Lett. **3**, 1067 (2003).
[7] A. Fujiwara *et al.*, Jpn. J. Appl. Phys. **40**, L1229 (2001).
[8] J. A. Misewich *et al.*, Science **300**, 783 (2003).
[9] M. Freitag *et al.*, Nano Lett. **4**, 1063 (2004).
[10] M. Freitag *et al.*, Phys. Rev. Lett. **93**, 076803 (2004).
[11] R. Martel *et al.*, Phys. Rev. Lett. **87**, 256805 (2001).
[12] L. Albert, Ph.D. thesis, Université de Montréal, 2005; R. Doyon, P. Nadeau, and P. Vallée, in *Imaging the Universe in Three Dimensions*, edited by W. van Breugel and J. Bland-Hawthorn, Astronomy Society Pacific Conference Series Vol. 195 (Astron. Soc. Pacific, US, 2000), p. 548.
[13] Adam *et al.* (to be published).
[14] This estimate assumes an isotropic emission and takes into account the angular acceptance ($\Omega = 0.0095$ sr), the optic losses, and the detector's relative sensitivity.
[15] M. Sveningsson *et al.*, Appl. Phys. Lett. **81**, 1095 (2002).
[16] S. M. Bachilo *et al.*, Science **298**, 2361 (2002).
[17] S. Lebedkin, F. Hennrich, T. Skipa, and M. M. Kappes, J. Phys. Chem. B **107**, 1949 (2003).
[18] J. W. Allen, J. Lumin. **48–49**, 18 (1991).
[19] H. Weman *et al.*, Semicond. Sci. Technol. **7**, B517 (1992).
[20] W. W. Piper and F. E. Williams, Phys. Rev. **98**, 1809 (1955).
[21] R. Chin *et al.*, Electron. Lett. **16**, 467 (1980).
[22] M. J. O'Connell *et al.*, Science **297**, 593 (2002).
[23] F. Wang, G. Dukovic, L. E. Brus, and T. F. Heinz, Phys. Rev. Lett. **92**, 177401 (2004).
[24] Y.-Z. Ma, L. Valkunas, S. M. Bachilo, and G. R. Fleming, J. Phys. Chem. B **109**, 15 671 (2005).
[25] F. Wang *et al.*, Phys. Rev. B **70**, 241403 (2004).
[26] Y.-Z. Ma *et al.*, Phys. Rev. Lett. **94**, 157402 (2005).
[27] C. Manzoni *et al.*, Phys. Rev. Lett. **94**, 207401 (2005).
[28] G. Dukovic *et al.*, Nano Lett. **5**, 2314 (2005).
[29] J. Chen *et al.*, Science **310**, 1171 (2005).